A Numerical Analysis of Condenser Performance of a Seawater Desalination System

by

Hassan Mohamed

Submitted to the Department of Mechanical Engineering in Partial Fulfillment of the Requirement for the Degree of

Bachelor of Science
at the
Massachusetts Institute of Technology

June 2009

Signature of Author.....
Department of Mechanical Engineering
May 8, 2009

Certified by.....
John H. Lienhard V
Collins Professor of Mechanical Engineering
Thesis Supervisor

Accepted by.....
John H. Lienhard V
Collins Professor of Mechanical Engineering
Chairman, Undergraduate Thesis Committee

A Numerical Analysis of Condenser Performance of Seawater Desalination System

by

Hassan Mohamed

Submitted to the Department of Mechanical Engineering
on May 8, 2009 in partial fulfillment of the
requirements for the Degree of Bachelor of Science in
Mechanical Engineering

Abstract

This thesis presents the numerical analysis of three type condensers for desalination of seawater system. The condensers that were analyzed were a finned tube condenser that was built in Malaysia desalination plant, a cooling tube condenser in Jordan, and a common plate finned tube condenser. The goal of the analysis is to observe the thermal performance parameters of a condenser such as heat and mass transfer coefficient, surface effectiveness and condensate flow rate. The parameters that were changed in the analysis were the face velocity of air, the water velocity, and the number of rows of tubes. The numerical analysis was done based on basic heat exchanger analysis using e-NTU method for a dry case, and using a j-factor correlation that was developed by McQuiston for studying the wet case.

Results from the basic heat exchanger analysis showed the air humidity ratio profile and temperature profile of air and water at the outlet of the condenser. The exit air temperature and humidity ratio were inversely proportional to the length of the condenser, whereas the temperature of the water at the outlet was proportional to the length of the condenser. Results from the j-factor correlation method show that the heat and mass transfer coefficient of the system increased when the number of rows of tubes, face velocity and water velocity increased. Similarly, the analysis showed that the condensate flow rate was highly influenced by the face velocity. In addition, the surface effectiveness was inversely proportional to the face velocity.

Thesis Supervisor: John H. Lienhard V
Title: Collins Professor of Mechanical Engineering

Acknowledgments

I would like to thank several people who have helped me tremendously with completing this thesis. First of all, I am very grateful to Professor John H. Lienhard V for all his help and guidance. It has been a great experience to work under his supervision as I have learned a lot about heat and mass transfer. In addition, I would like to thank Manikandan Mathur for offering Matlab assistance. Finally, I must thank to all my family members for their relentless support throughout my academic years

1. Introduction

In a solar-driven humidification-dehumidification desalination seawater system, there are three main components which are a solar collector, a humidifier and a condenser. A condenser is the final component of the system. It is a heat exchanger that condenses hot vapor into pure water. Two typical and widely used condensers are cooling tubes and finned condensers. They both have been used experimentally in a pilot and bench desalination system in Jordan and Malaysia.

This thesis will numerically study the performance of a condenser by using heat exchanger analysis, ε-NTU method, for a dry case and also by using j-factor correlation for a wet case. The goal of the study is to theoretically observe the thermal performance of the condenser such as heat and mass transfer coefficients, surface effectiveness and condensate flow rate by controlling face velocity of air and the water velocity. The numerical process will also predict the temperature profile of the condenser and estimate the temperature output for a given inlet specification of the condenser.

2. Nomenclature

A_c	Cross sectional area (m^2)
A_0	Total heat transfer area (m^2)
A_{fin}	Fin area (m^2)
A_{free}	Free flow area (m^2)
A_{front}	Heat exchanger frontal area (m^2)
A_{tube}	Tube surface area (m^2)
$c_{p,a}$	Specific heat of air (kJ/kgK)
D_i	Tube inside diameter (m)
D_h	Hydraulic diameter (m)
D_o	Tube outside diameter (m)
f	Fanning friction factor
f_h	Fin height (m)
δ	Fin thickness (m)
G_c	Mass flux based on free flow area (kg/m^2s)
h_{ad}	Heat transfer coefficient for dry side (W/m^2K)
h_{aw}	Heat transfer coefficient for wet side (W/m^2k)
h_m	Mass transfer coefficient (kg/m^2s)
i_{fg}	Latent heat of water vapor
j	Colburn j-factor
k_{air}	Thermal conductivity of air (W/mK)
k_{tube}	Thermal conductivity of tube (W/mK)
l	Tube length (m)
Le	Lewis number
$\dot{m}_a$	Air mass flow rate (kg/s)
$\dot{m}_w$	Water mass flow rate (kg/s)
$\dot{m}_{wm}$	Condensate flow rate (kg/s)
N	Number of total tubes
P	Perimeter (m)

Pr	Prandtl number
p_v	Vapor pressure (Pa)
p_0	Atmospheric pressure (Pa)
q_s	Sensible heat transfer rate (W)
R_{ad}	Air Side dry thermal resistance (K/W)
R_{adfin}	Air Side dry thermal resistance with fin (K/W)
R_{aw}	Air-side wet thermal resistance (K/W)
Re_D	Reynolds number based on tube diameter
Re_δ	Reynolds number based on fin thickness
R_{tube}	Tube thermal resistance (K/W)
R_{water}	Water-side thermal resistance (K/W)
Sc	Schmidt number
t	Fin Thickness (m)
T_{a1}	Temperature of air at heat exchanger inlet (K)
T_{a2}	Temperature of air at heat exchanger outlet (K)
T_{sa1}	Tube wall temperature on the air side at the heat exchanger inlet (K)
T_{sa2}	Tube wall temperature on the air side at the heat exchanger outlet (K)
T_{sw1}	Tube wall temperature on the water side at the heat exchanger inlet (K)
T_{sw2}	Tube wall temperature on the water side at the heat exchanger outlet (K)
T_{w1}	Temperature of water at heat exchanger inlet (K)
T_{w2}	Temperature of water at heat exchanger outlet (K)
U	Overall heat transfer coefficient (W/m^2K)
U_{face}	Heat exchanger face velocity (m/s)
x	Mass fraction (%)
x_a	Tube longitudinal distance (m)
x_b	Tube transverse distance (m)
ρ_a	Density of air at heat exchanger inlet (kg/m^3)
μ_a	Dynamic viscosity of air at heat exchanger inlet (kg/ms)
η	Heat exchanger surface effectiveness
ϕ	Heat exchanger efficiency
ω_{a1}	Humidity ratio of air at T_{a1} (kg water/ kg air)
ω_{a2}	Humidity ratio of air at T_{a2} (kg water/ kg air)
ω_{sa1}	Humidity ratio of air at T_{sa1} (kg water/ kg air)
ω_{sa2}	Humidity ratio of air at T_{sa2} (kg water/ kg air)
ΔT_{lm}	Log mean temperature difference (K)
$\Delta\omega_{lm}$	Log mean humidity ratio difference (kg water/kg air)

3. Analysis

Three different condensers were analyzed in this paper. Two of them were the existing cooling condensers in desalination plants in Malaysia and Jordan [10]. Another condenser that was analyzed was a basic finned tube condenser with multiple tubes.

Figure 1a shows the dehumidifier that was built in Malaysia. It was a 3 m long cylinder made from galvanized steel plates with a diameter of 170 mm. It has ten longitudinal fins on the outside surface and nine fins in the inside cylinder. The height of the fin was 50 mm and the thickness was 1.0 mm. A 9.5 mm copper tube was attached to the condenser. The condenser is fixed vertically in a 316 mm diameter PVC pipe. The condenser in Jordan [Figure 1b] was built from 2.0 x 1.0 m galvanized steel plates for the pilot plant. The tube is made of copper and it has 11 mm outside diameter and 18 m long. It as welded to a galvanized plate in a helical shape. The condenser was fixed vertically in a rectangular conduit of the desalination unit.

Figure 2 shows the typical finned cooling tubes condenser that consists of multiple tubes of water and several plate fins. There is cross flow interaction between the water and air. This paper analyzed to type of finned cooling tubes which are 4 rows 15 fins per inch. Both condensers were analyzed using the basic heat exchanger analysis with ε-NTU method that is explained in later in the paper. Due to complexity of geometrical shape and insufficient information of the dimensions of both condensers, the wet condition analysis was not applied. However, the wet condition analysis was still applied on the typical in order to determine the important parameters that control the condenser performance.

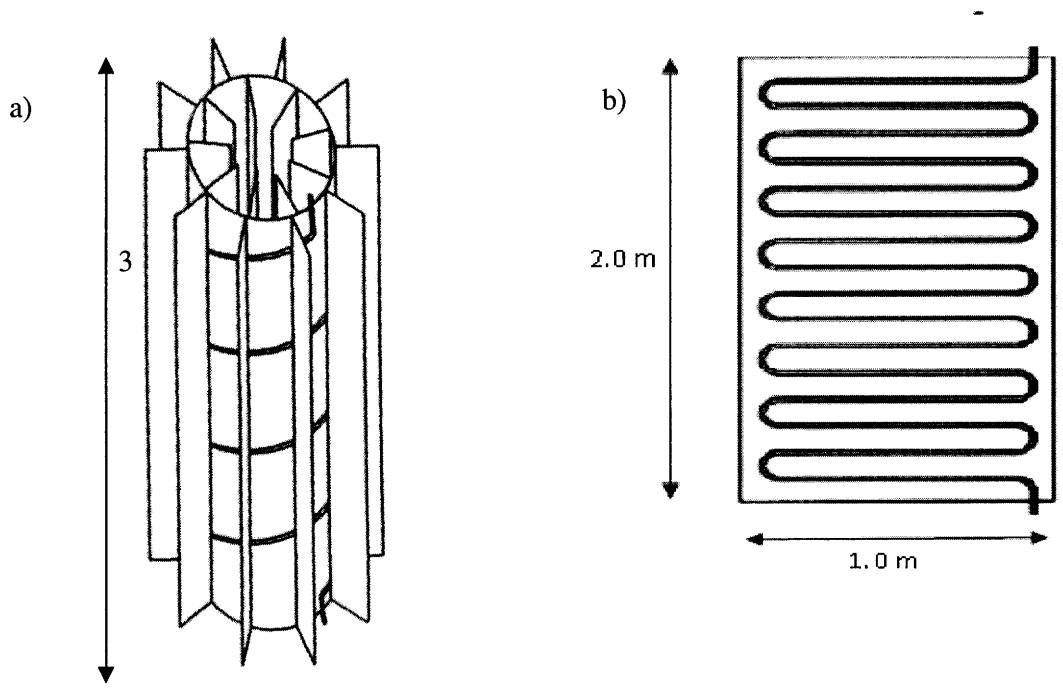

Figure 1: a) Finned tube circular condenser in Malaysia. b) Cooling tube condenser in Jordan.

c)

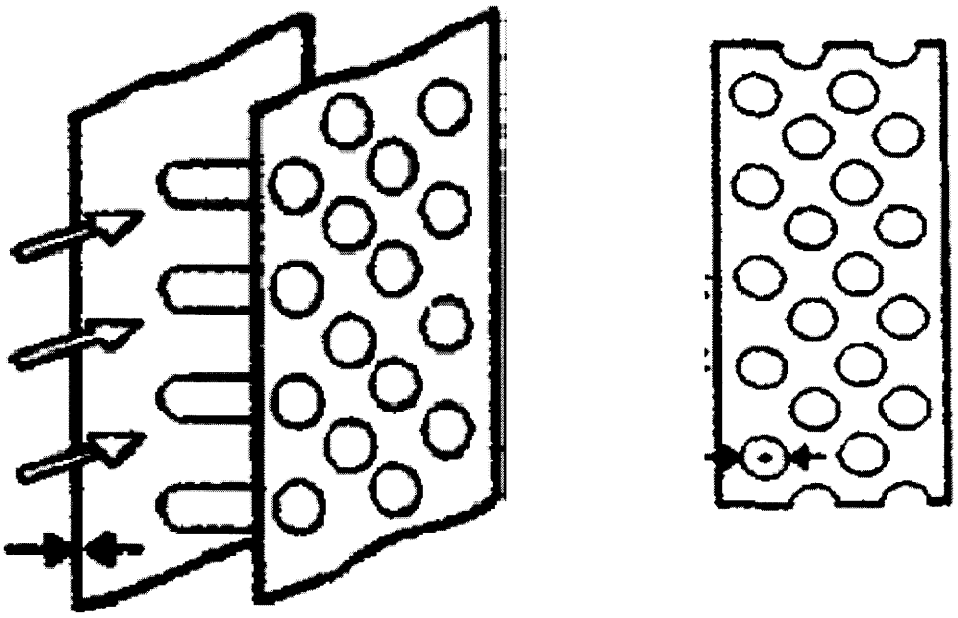

Figure 2: Plate Finned Tube Condenser.

3.1 Dry Case

A heat transfer coefficient of the condenser can be evaluated from the basic heat transfer analysis with a resistance circuit diagram. Heat transfer mechanisms that were mainly involved in the process are only convection and conduction while radiation is assumed to be negligible. For a cooling tube condenser, the resistance circuit diagram is shown in Figure 3.

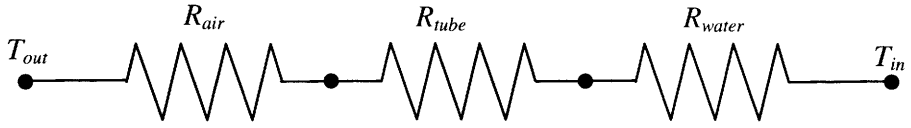

Figure 3: Resistance circuit diagram for cooling tube condenser.

The total heat resistance, R_{total}, is calculated in Eqn. 1 below:

$$R_{total} = R_{ad} + R_{tube} + R_{water} \tag{1}$$

The effective resistance consists of resistance of the air, R_{air}, the resistance of the condenser wall, R_{tube}, and the resistance of the seawater, R_{water}. All the resistances can be expressed as a

function of thermal conductivity of the condenser wall, k, or heat transfer coefficient, h as shown in Eqns. 2, 3, and 4 below.

$$R_{ad} = \frac{1}{h_{air}A} \tag{2}$$

$$R_{tube} = \frac{\ln (D_o/D_i)}{2\pi k_{tube} lN} \tag{3}$$

$$R_{water} = \frac{1}{h_{water}A} \tag{4}$$

In the Eqn. 2, since the condensers are enclosed in a rectangular and circular pipe, the heat transfer coefficient at the air side of the condenser can found by using Nusselt number equation of a forced flow in a pipe as shown in Eqn. 5 below.

$$Nu_D = \frac{\left(\frac{f}{8}\right)(Re_D - 1000)Pr}{1 + 12.7\sqrt{\frac{f}{8}}(Pr^{2/3} - 1)} \tag{5}$$

where the friction factor, f is,

$$f = \frac{1}{(1.82 \log_{10} Re_D - 1.64)^2} \tag{6}$$

and the Reynolds number, Re_D is defined in Eqn. 7,

$$Re_D = \frac{\rho_a U_{face} D_h}{\mu_a} \tag{7}$$

The hydraulic diameter, D_h, of the passage of air side is expressed as below,

$$D_h = \frac{4A_c}{P} \tag{8}$$

where for the finned tube circular condenser in Malaysia the hydraulic diameter depends on the circular PVC pipe, whereas for the cooling tube condenser in Jordan its hydraulic diameter

depends on the rectangular passage of the air side. With the calculated Nusselt number, *Nu*, the heat transfer coefficient for the air side can be obtained by using expression below.

$$h_{ad} = \frac{Nuk_{air}}{L} \tag{9}$$

Previous work used Dittus-Boelter correlation for estimating the heat transfer coefficient at the water side. However in this analysis, the correlation given by Wagnick (1995) [4] was used to calculate the heat transfer coefficient of seawater. The heat transfer coefficient for sea water inside tube is shown in Eqn. 10.

$$h_{water} = (3293.5 + T_w(84.24 - 0.1714T_w) - x(8.471 + 0.1161x + 0.2716T_w))/ ((\delta_i/0.01727)^{0.2})((0.656V)^{0.8})(\delta_i/\delta_o). \tag{10}$$

The mass fraction of salt, x that was used in the analysis was estimated around 3.5 %. For a fin tube condenser, the effect of the fin is taken into account into the total thermal resistance as shown in Figure 4 below.

Figure 4: Resistance circuit diagram for fin condenser.

In Figure 4, the resistance due to air only is replaced with the resistance of the air and fins where the air resistance is now expressed as functions of heat transfer coefficient and surface effectiveness of the fins as shown in Eqn. 11.

$$R_{adfin} = \frac{1}{\eta h_{air} A} \tag{11}$$

,

The surface effectiveness is defined as below,

$$\eta = 1 - \frac{A_f}{A_0}(1 - \phi) \tag{12}$$

where fin efficiency, ϕ can be calculated as,

$$\phi = \frac{\tanh [ml]}{ml} \tag{13}$$

and m is defined as,

$$m^2 = \frac{hP}{k_{tube}A_c} \tag{14}$$

For a finned tubes condenser, the effective resistance needs to consider for both tube surfaces that have fins and without fins. Thus the effective thermal resistance of the fins is analogically presented in parallel as shown in Figure 5, and it can be calculated using Eqn. 15.

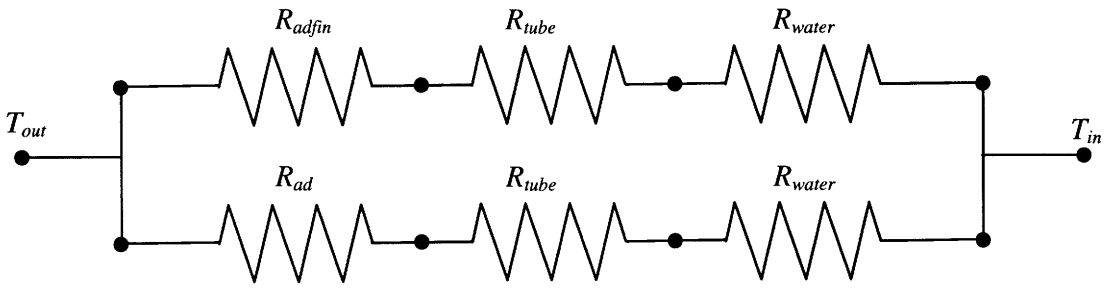

Figure 5: Resistance circuit is arranged in parallel for effective thermal resistance.

$$R_{effective} = \frac{(R_{ad} + R_{tube} + R_{water})(R_{adfin} + R_{tube} + R_{water})}{(R_{adfin} + R_{air} + 2R_{tube} + 2R_{water})} \tag{15}$$

By knowing the effective thermal resistance of the system, the overall heat transfer coefficient can be obtained from Eqn. 14 where it is expressed as a function of effective thermal resistance and total area.

$$U = \frac{1}{R_{effective}A_o} \tag{16}$$

Besides, other conditions of the condenser such as temperature outlet for the air and water can be predicted by applying ε-NTU relationships as shown in Eqns. 17, 18, 19 and 20 below.

$$NTU = \frac{UA}{C_{min}} = \frac{R}{C_{min}} \tag{17}$$

$$\varepsilon_{cond} = \frac{1 - e^{-NTU(1-C_{cr})}}{1 - C_{cr}e^{-NTU(1-C_{cr})}} \tag{18}$$

$$T_{air\ out} = T_{air\ in} - \frac{\varepsilon_{cond} C_{min}(T_{air\ in} - T_{water\ in})}{C_{hot}} \tag{19}$$

$$T_{air\ out} = \frac{\varepsilon_{cond} C_{min}(T_{air\ in} - T_{water\ in})}{C_{cold}} + T_{water\ in} \tag{20}$$

With the predicted temperature profile across the length of the tube condenser, the humidity ratio can be obtained by using Eqn. 21 below.

$$\omega = 0.622\left(\frac{p_v}{p - p_v}\right), \tag{21}$$

where the vapor pressure for each different temperature can be calculated from a given correlation [1] below.

$$c_1 = -5.8002206 \times 10^3$$
$$c_2 = 1.3914993$$
$$c_3 = -4.8640239 \times 10^{-2}$$
$$c_4 = 4.1764768 \times 10^{-5}$$
$$c_5 = -1.4452093 \times 10^{-8}$$
$$c_6 = 6.5459673$$

$$p_v = \exp\left[\frac{c_1}{T} + c_2 + c_3 T + c_4 T^2 + c_5 T^2 + c_6 \ln(T)\right] \tag{22}$$

For the dry condition analysis, the temperature profile of the condenser across the length of the condenser as well as the air humidity ratio of the in the condenser is plotted. The analysis of the temperature profile and can be used as a good rough approximation of the overall heat transfer coefficient of the condenser, the temperature outlet of the air and water sides. This dry condition analysis however can only be used with an assumption that no condensation occurs. Section 3.1.1 and 3.1.2 give the detailed dimensions and inlet specification for both condensers as used in the analysis.

3.1.1 Finned tube condenser (Malaysia)

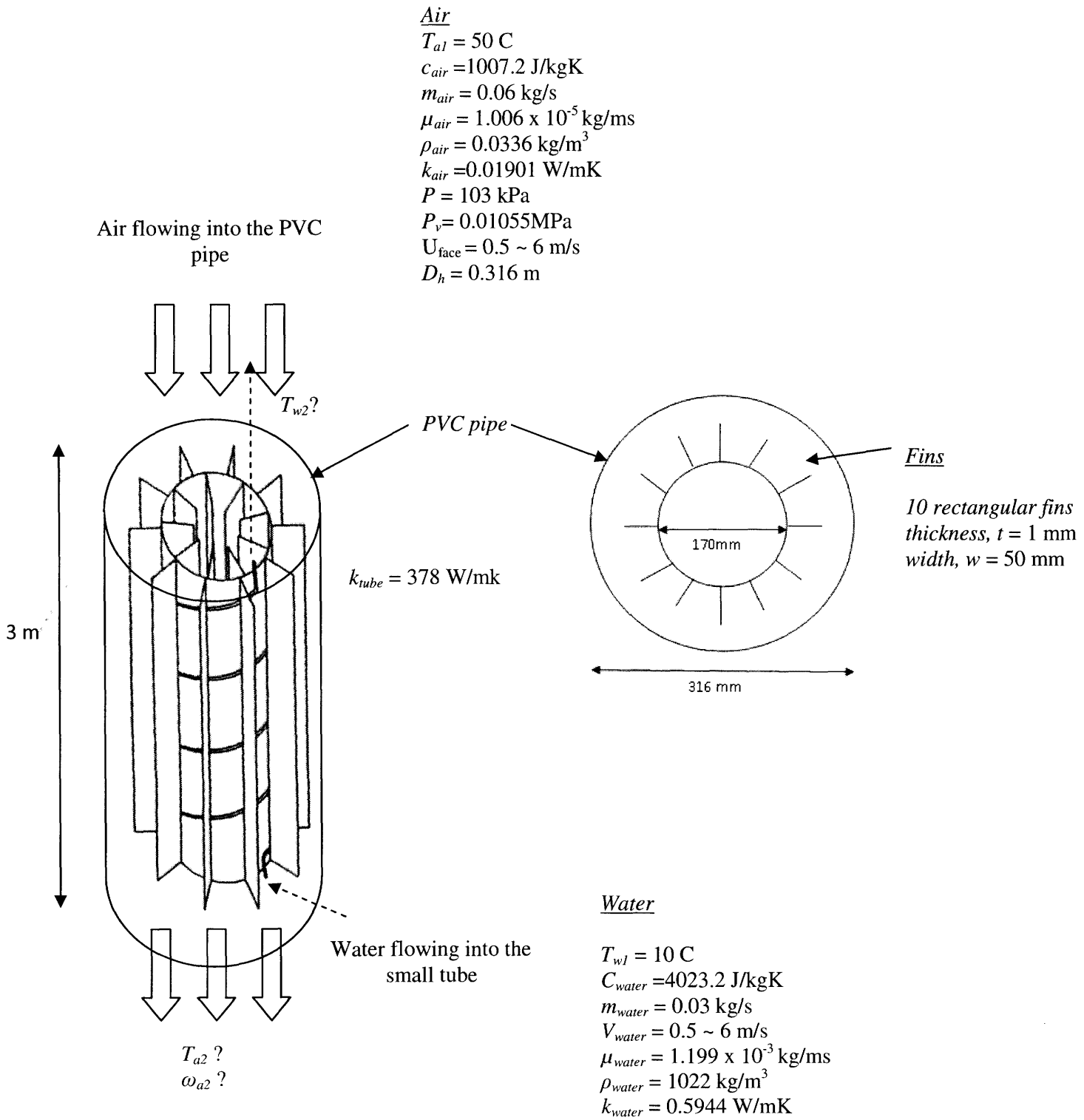

Figure 6: Finned tube circular condenser in Malaysia with inlet condition of water and air.

3.1.2 Cooling Tube condenser (Jordan)

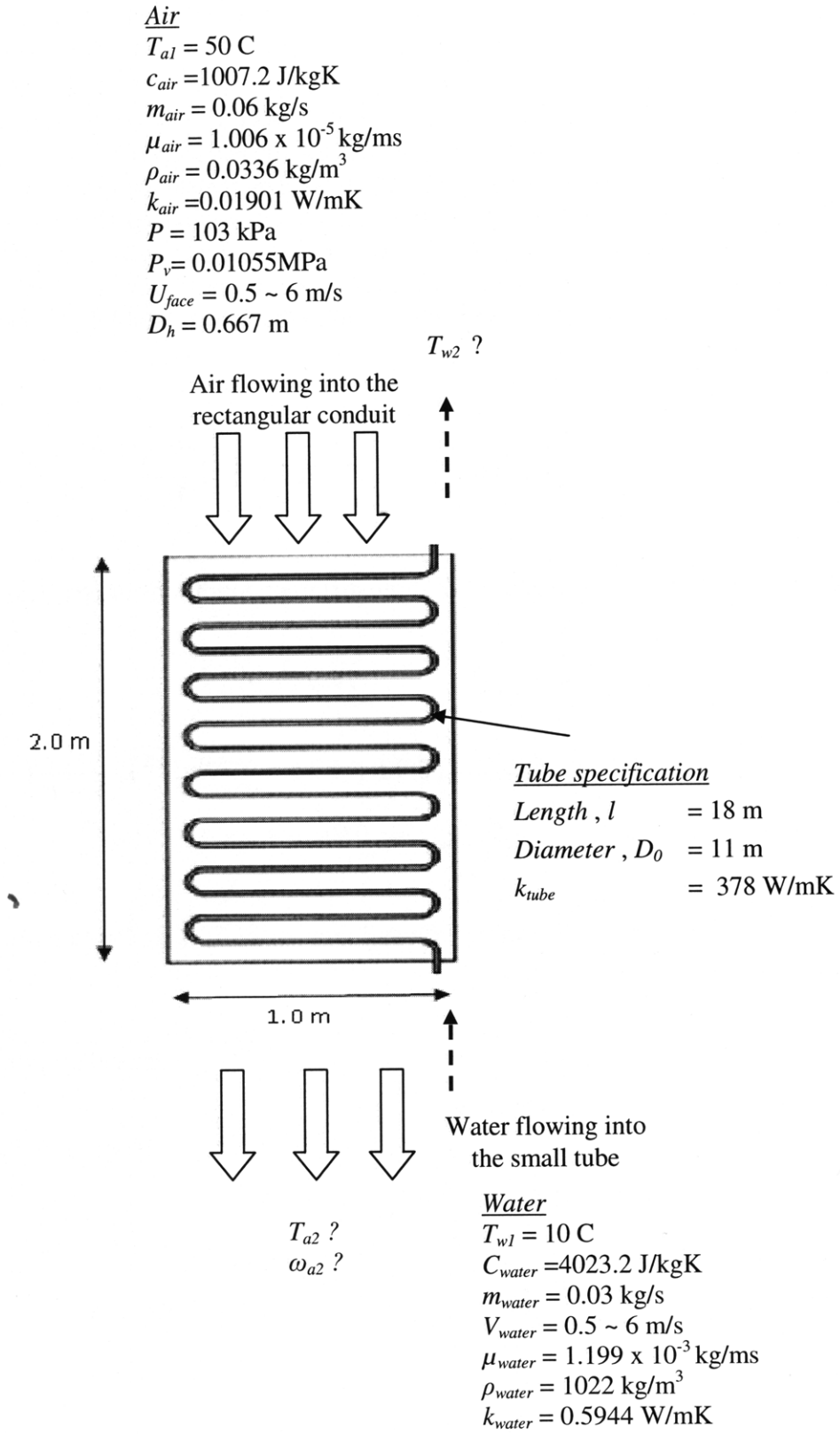

Figure 7: Cooling tube condenser in Jordan with inlet condition of water and air

3.2 Wet case

For the wet condition analysis, where condensation occurred on the wall surface of the condenser, the basic heat exchanger analysis which was shown previously cannot be used to analyze the process. To better approach the wet condition problem of the condenser, the combined effect heat and mass transfer process need to be taken into account. A film layer and droplets of condensed water were formed on the surface of the fins. Thus, the overall heat transfer coefficient was expected to be changed. The resistance of the conduction of the tube wall and the convection of the water were calculated similar to dry cases as shown previously. However the resistance of the air side was found differently as the latent heat of condensation was considered in the fin surface effectiveness. The heat transfer coefficient of the air for wet condition, h_{aw} is estimated using the latent-j factor correlation for sensible heat developed by McQuiston [6,7].

$$j_s = 0.00014 + 0.2618 Re_D^{-0.4} \left(\frac{A}{A_{tb}}\right)^{-0.15} f_s(\delta) \tag{23}$$

Here, the fanning friction factors for three different conditions are expressed below.

$$f_{dry} = 1.0 \tag{24}$$

$$f_{dropwise} = \left(0.90 + 4.3 \times 10^{-5} Re_\delta^{1.25}\right)\left(\frac{\delta}{\delta - t}\right)^{-1} \tag{25}$$

$$f_{filmwise} = 0.84 + 4.0 \times 10^{-5} Re_\delta^{1.25} \tag{26}$$

To calculate the Reynolds number, Re and area ratio, A/A_{tb} in the fanning -factor , Eqns. 27 – 29 are used.

$$Re_D = \frac{G_c D}{\mu_a} \quad \text{based on tube outer diameter} \tag{27}$$

$$Re_\delta = \frac{G_c \delta}{\mu_a} \quad \text{based on tube fin spacing} \tag{28}$$

$$\frac{A}{A_{tb}} = \frac{4}{\pi}\frac{x_a}{D_h}\frac{x_b}{D}\sigma_f, \tag{29}$$

where the mass flux, G_c is defined as Eqn. 30 below.

$$G_c = \frac{\rho_a A_{front} U_{face}}{A_{free}} \tag{30}$$

The latent-j correlation can be used to estimate three different conditions, dry, dropwise and film wise condensation. The heat transfer dimensionless parameter is used to find the heat transfer, h_a and mass transfer coefficient, $h_{m,a}$ of the air side by using expression below.

$$j_s = \frac{h_a}{G_c c_{p,a}} Pr_a^{2/3} \tag{31}$$

$$j_s = \frac{h_{m,a}}{G_c} Sc_a^{2/3} \tag{32}$$

With the heat transfer coefficient obtained for the air side, the overall heat transfer coefficient can be obtained by using Eqn. 16 where the new heat transfer coefficient for wet surface, h_{aw} is replaced in the equation for the air side, and the surface effectiveness is approximated around 0.9 before the actual surface effectiveness calculation that would be shown later. The exit temperature of air, T_{a2} and water T_{w2} was estimated by using energy balanced for sensible heat below [6].

$$\dot{q}_s = \dot{m}_a c_p (T_{a1} - T_{a2}) = UA_0 (LMTD) \tag{33}$$

$$LMTD = \frac{(T_{a1} - T_{a2}) - (T_{w1} - T_{w2})}{\ln\left(\frac{(T_{a1} - T_{a2})}{(T_{w1} - T_{w2})}\right)} \tag{34}$$

By knowing the inlet conditions such as temperature of the water and air, a double iteration process can be applied by using a computer program that is more complex such as Matlab instead of using MathCad in previous calculation. Later, the wall temperature for air and water side is obtained using Eqn. 35 and Eqn. 36.

$$\frac{T_{w1} - T_{sw1}}{R_{water}} = \frac{T_{sw1} - T_{sa1}}{R_{tube}} = \frac{T_{sa1} - T_{a1}}{R_{air}} \tag{35}$$

and for the outlet condition,

$$\frac{T_{w2} - T_{sw2}}{R_{water}} = \frac{T_{sw2} - T_{sa2}}{R_{tube}} = \frac{T_{sa2} - T_{a2}}{R_{air}} \tag{36}$$

After obtaining every temperature condition, the humidity ratio of air, ω can be obtained by using Eqn. 21 and Eqn. 22 as previously shown in dry condition section. When the estimated temperature and humidity ratio outlet are found, the surface effectiveness of the fins was calculated again by using Eqn. 12. Nevertheless, the new value of M this time takes in to account the effect of the latent heat of condensation of water vapor on the wall. The efficiency of fins is defined in terms of the in terms of fin height and new M as shown below.

$$\phi = \frac{\tanh\left[Mf_h\right]}{Mf_h} \tag{37}$$

The value of M [6] is no longer a constant because it depends on the humidity ratio on the wall and the latent heat of vaporization. Eqn. 38 shows the expression of M,

$$M^2 = \left(\frac{2h_a}{k_{tube}t}\right)\left(1 + \frac{Ci_{fg}}{c_{p,a}Le^{2/3}}\right), \tag{38}$$

where in this analysis, Le = 1 as the heat and mass transfer was assumed to be unity. The C is constant [7] which was calculated below,

$$C = \frac{C_1 + C_2}{2} \tag{39}$$

where,

$$C_1 = \frac{\omega_{a1} - \omega_{sa1}}{T_{a1} - T_{sa1}} \quad , \quad C_2 = \frac{\omega_{a2} - \omega_{sa2}}{T_{a2} - T_{sa2}} \tag{40}$$

The new value of surface effectiveness can replace the assumption value in the overall heat transfer equation. Thus the iteration process of Eqn. 33 can be repeated again to find the new value of temperature outlet. The process of finding surface effectiveness and temperature outlet can be repeated until both values agree. Since the condensate flow rate the condensate mass cannot be obtained experimentally, it was estimated by using Eqn. 41 below

$$\dot{m}_{wm} = A_0 \eta h_{m,a} (\Delta\omega_{lm}) \tag{41}$$

,

where log mean humidity ratio difference, $\Delta\omega_{lm}$ is defined as follows.

$$\Delta\omega_{lm} = \frac{(\omega_{a1} - \omega_{sa1}) - (\omega_{a2} - \omega_{sa2})}{ln\left(\frac{\omega_{a1} - \omega_{sa1}}{\omega_{a2} - \omega_{sa2}}\right)} \tag{42}$$

Section 3.2.1 gives the details of the plate-fined-tube condenser that was used in the wet condition analysis as well as the water and air inlet specification. The effects of varying air face velocity, U_{face} on the surface heat transfer coefficient, surface effectiveness and condensate flow rate were observed. In addition, the velocity of the air as well as the temperature inlet was also examined in this analysis.

3.2.1 Plate-Finned-tube condenser

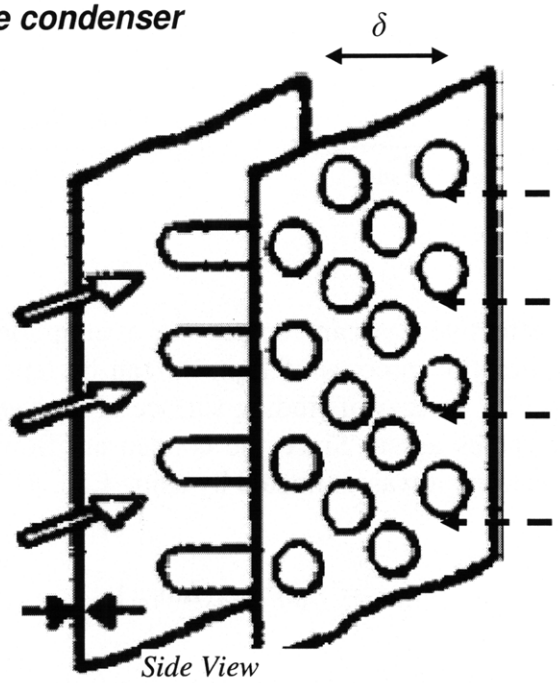

Figure 8: Plate finned tube condenser with inlet condition of air and water

Table 1: Dimensional parameters for the 4 row and 5 row finned tube condenser

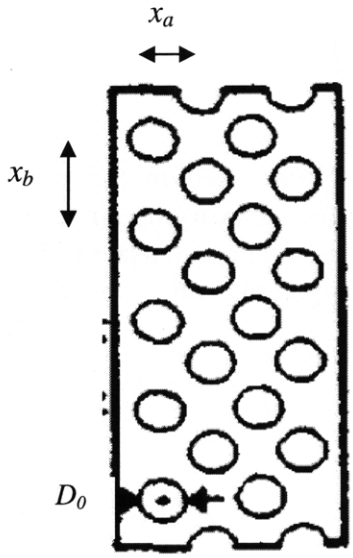

Parameter	*4- Rows*	*5-Rows*
Tube outside Diameter (m)	0.00819	0.00819
Streamwise tube distance, x_a (m)	0.01588	0.01588
Transverse tube distance, x_b (m)	0.02540	0.02540
Fin Thickness, f_t (m)	0.00013	0.00013
Fin Spacing, fs (m)	0.00169	0.00169
Equivalent Fin height, f_h (m)	0.00940	0.00940
Frontal Area, A_{front} (m)	0.16645	0.20806
Free Flow Area, A_{free} (m)	0.10031	0.13056
Ratio of Free Flow to Frontal Area	0.60262	0.62750
Tube Surface Area, A_{tube} (m^2)	0.67112	1.07485
Fin Surface Area, A_{fin} (m^2)	10.8655	11.3296
Total Effective Area, A_0 (m^2)	11.5366	12.4044
Hydraulic Diameter, D_h (m)	0.00221	0.00334

4. Results

4.1 Dry Condition Analysis

4.1.1 Finned Tube Circular Condenser (Malaysia)

Figure 9a and 9b below show the temperature profile of the finned tube circular condenser for both air and water sides across the height which is 3m.

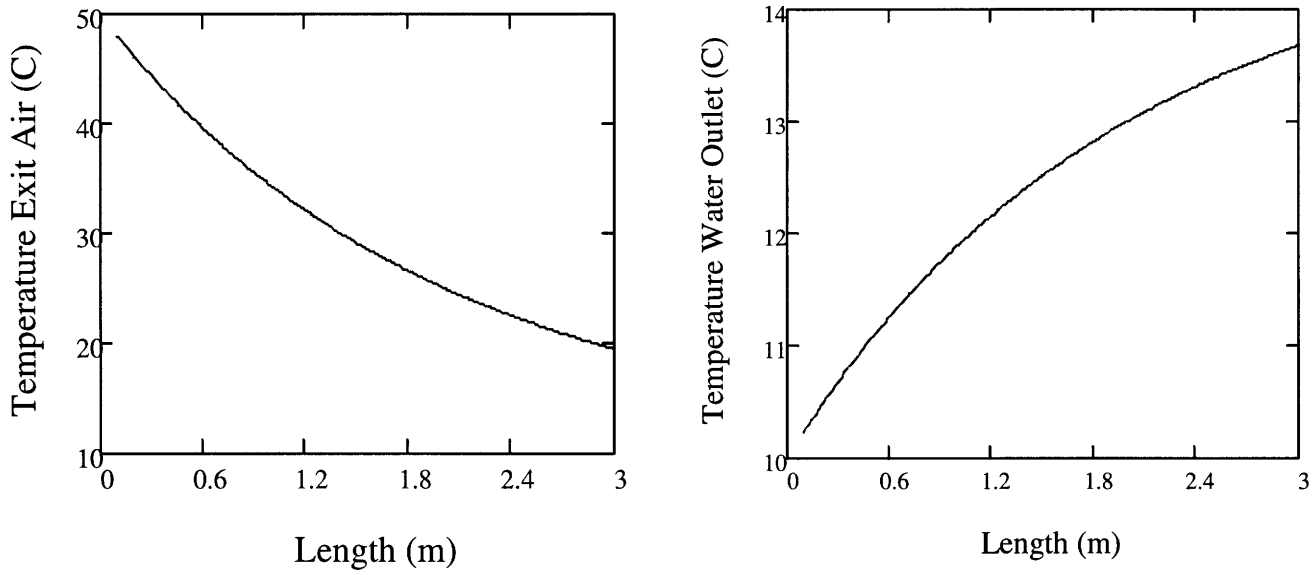

Figure 9: a) Temperature profile of exit air along the height. b) Temperature profile of exit water in terms of the height of the condenser.

In Figure 9a, the curve shows that the temperature of the air decreases along the height. The air temperature at the exit was estimated to be 21.3 C. For the water, Figure 9b shows that the temperature of the water increases till it achieve approximately 13.8° C at the exit temperature. The estimated temperature at every point of length was used to find the humidity ratio profile. Figure 10 below shows the humidity ratio profile along the height of the condenser.

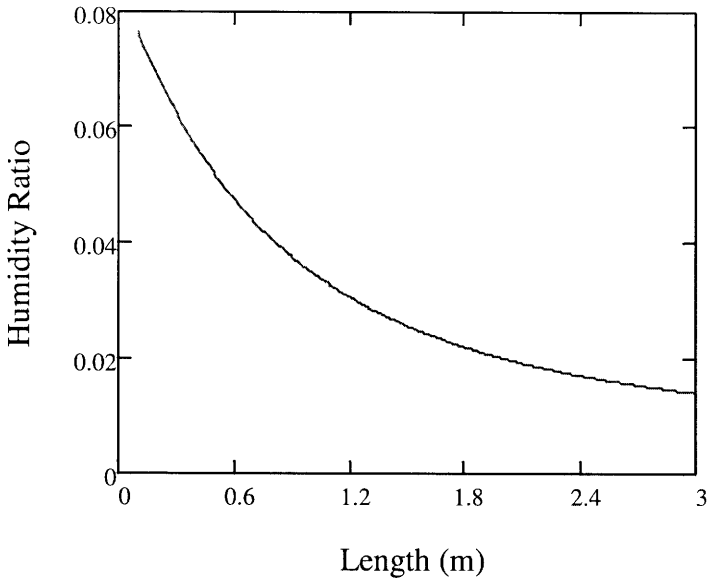

Figure 10: Humidity ratio profile for finned tube circular condenser (Malaysia)

The graph shows that the humidity ratio of air decreases along the circular condenser. The decreasing value of humidity ratio shows that there was some water from the air was condensed during the cooling process. This dry analysis could not predict the condensed water flow rate. It, however, gives some rough approximation of how much humidity ratio at the exit condenser how much possible water has been extracted along the height. The humidity ratio at the air outlet was estimated around 0.015.

4.1.2 Cooling Tube condenser (Jordan)

Figure 11a and 11b below show the temperature profile of the cooling tube condenser (Jordan) for both air and water sides along the length of the tube which is 19.2m

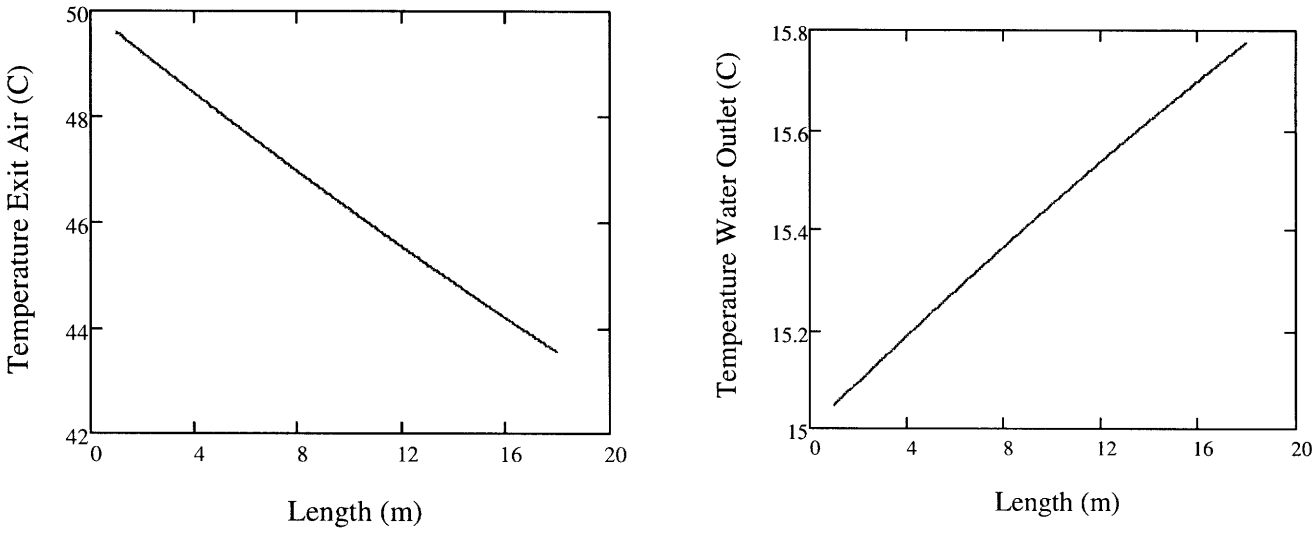

Figure 11: a) Temperature profile of exit air along the length. b) Temperature profile of exit water in terms of the length of the cooling tube condenser.

The graph in Figure 11a shows that the air temperature decreases almost linearly with the length of the tube. The temperature drop however is really small since the exit air temperature was only around 43.8°C. The curve in figure 4b shows that the water temperature increases as the water travels along the cooling tubes. The exit temperature was predicted to be around 15.7 °C. This cooling tube condenser has much lower temperature drop compared to the finned tube condenser. The lower temperature drop was expected to happen because the effect of not having fins. Without fins, the cooling process is much less efficient. As a result the exit temperature of both air and water do not change significantly from their inlet temperature. This result explains that the effect of having fins may give significant improvement to the performance of the condenser in cooling down the air and possibly condensing more water from the air. The temperature of each point of the length was used to find the humidity ratio of the air. Figure 12 below shows the humidity ratio profile along the length of the cooling tubes.

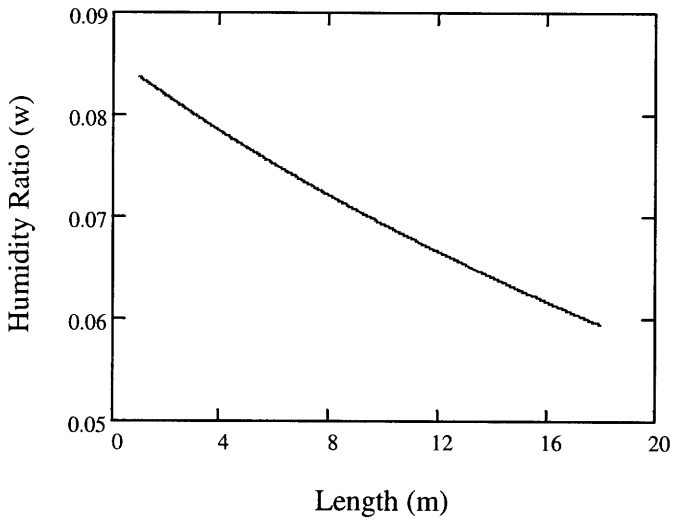

Figure 12: Humidity ratio profile for cooling tube condenser (Jordan)

The humidity ratio curve is decreasing along the length as the air temperature decreasing. The humidity ratio at the exit of the cooling tubes was estimated around 0.058 which was slightly higher compared to the humidity ratio at the exit of the finned tube circular condenser (Malaysia). This was expected since the temperature of air at the tube outlet was higher than the one of the Malaysia condenser.

4.2 Wet Condition Analysis

4.2.1 Finned Tube Condenser with multiple tubes

The wet condition analysis discovered the effect of face velocity on the j-factor, air heat transfer coefficient, surface effectiveness and condensate flow rate that would be presented in graphs below. The analysis also studied the influence of water velocity to the overall heat transfer coefficient. Figure 13 shows the j-factor for at three different conditions, dry, filmwise and dropwise condensation for 4 rows and 5 rows plate finned tube condenser. Figure 14 shows the air heat transfer coefficient that was obtained from the j-factor correlation.

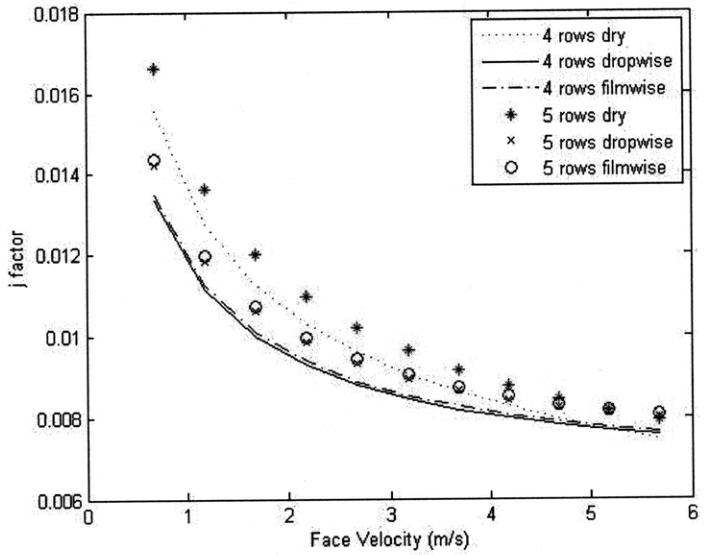

Figure 13: *j*-factor at three conditions: dry, dropwise and filmwise for 4 rows and 5 rows tubes configuration.

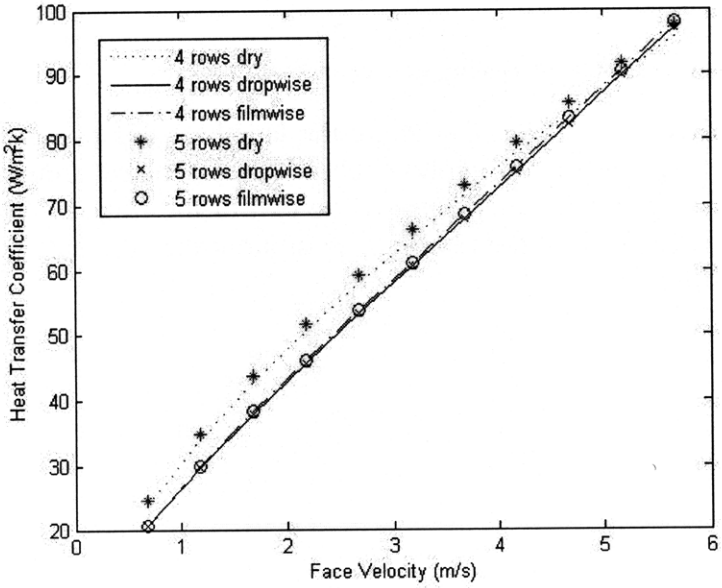

Figure 14: *j*-factor at three conditions: dry, dropwise and filmwise for 4 rows and 5 rows tubes configuration.

In Figure 13, the j-factor for each different condition decreases as the air face velocity increases. In Figure 14, all the curves show increment as the face velocity increases. The plotted curves for 5 rows configuration has a slightly 2.5% larger heat transfer coefficient value than the 4 rows configuration. The graph also shows that for dry condition the heat transfer coefficient is relatively higher compare to the heat transfer coefficient of the dropwise and filmwise conditions. This might be true since because the droplets and film layer that were form on the condenser wall during condensation have increased the thermal resistance on the air side. Subsequently, the effect of mass transfer decreases the heat transfer coefficient of the air. The heat transfer coefficient of the dropwise case seemed lower than of the filmwise condition. This might be because of the non uniform water droplets formed that created heat transfer variation accros the surface area. Nevertheless, the difference between the heat transfer coefficient of the dropwise and filmwise condition was still very small with 0.98% difference. The effect of the face velocity on the mass transfer coefficient was also studied. Figure 8 below shows the mass transfer coefficient vs. the face velocity of the water for both 4 rows and 5 rows.

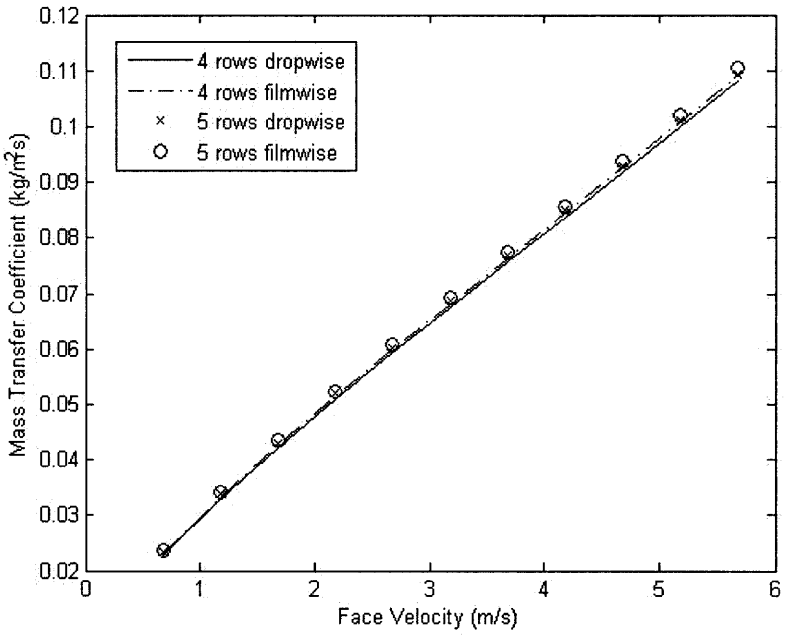

Figure 15: Mass transfer coefficient versus face velocity at dropwise and filmwise condtion for 4 rows and 5 rows configuration.

Figure 15 explains that the mass transfer coefficient for every condition increases as the face velocity increases. Like heat transfer curves, the mass transfer coefficient curves of five rows configuration are slightly larger than of the four rows configurations. The difference between the dropwise and filmwise conditions was also small with less than 1 % percentage difference. Later, Figure 16 below shows the effect of water velocity on the overall heat transfer coefficient.

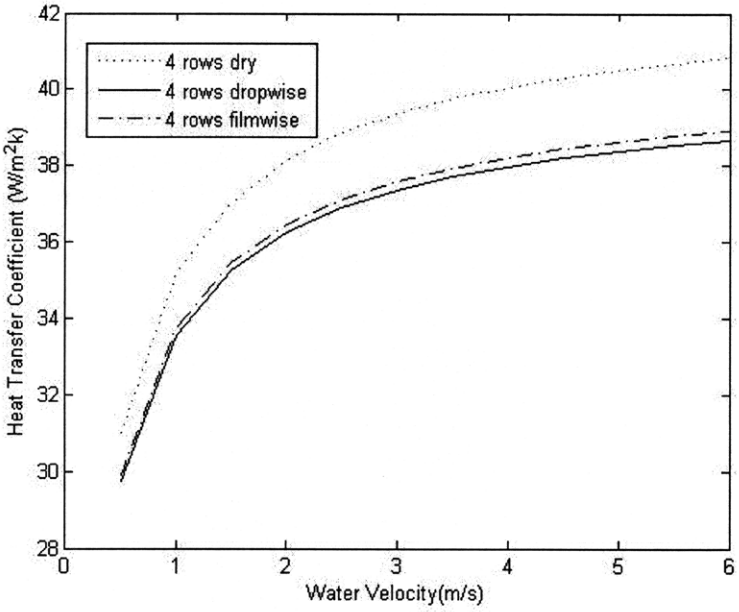

Figure 16: Overall heat transfer coefficient versus water velocity curves for dry, dropwise and filmwise conditions. (at 4 rows configuration and U_{face} = 3 m/s)

Figure 16 shows that the overall heat transfer coefficient of the system increases as the velocity of water increases. This was true due to the fact that the heat transfer coefficient of water was increased. The heat transfer coefficient increase quite linearly at the beginning before the increment slows down after about 2 m/s of water velocity. Again, this graph clearly shows that the dry condition has a better heat transfer coefficient since for dropwise and filmwise condition, an extra thermal resistance layer was formed and reduced the heat transfer coefficient. Besides the water velocity effect on the overall heat transfer coefficient, the face velocity of water has also affected the surface effectiveness of the fins. Figure 17 below shows the effect of face velocity of air on the surface effectiveness.

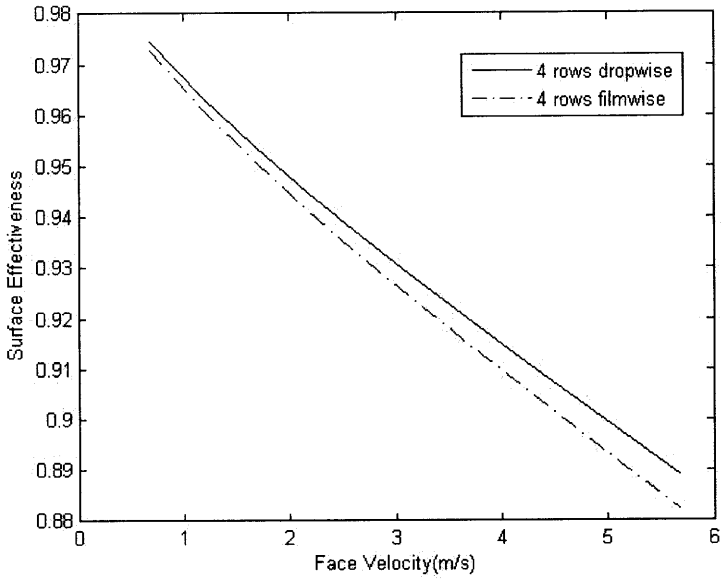

Figure 17: Surface effectiveness versus face velocity of air for 4 rows dropwise and filmwise conditions.

In Figure 17, the graph shows that for both dropwise and filmwise condition, the surface effectiveness decreases as the face velocity increases. The dropwise condition has slightly higher surface effectiveness than the filmwise condition has. The condensate flow rate also really depends on the face velocity of the air. Figure 18 shows the effect of face velocity on the condensate flow rate.

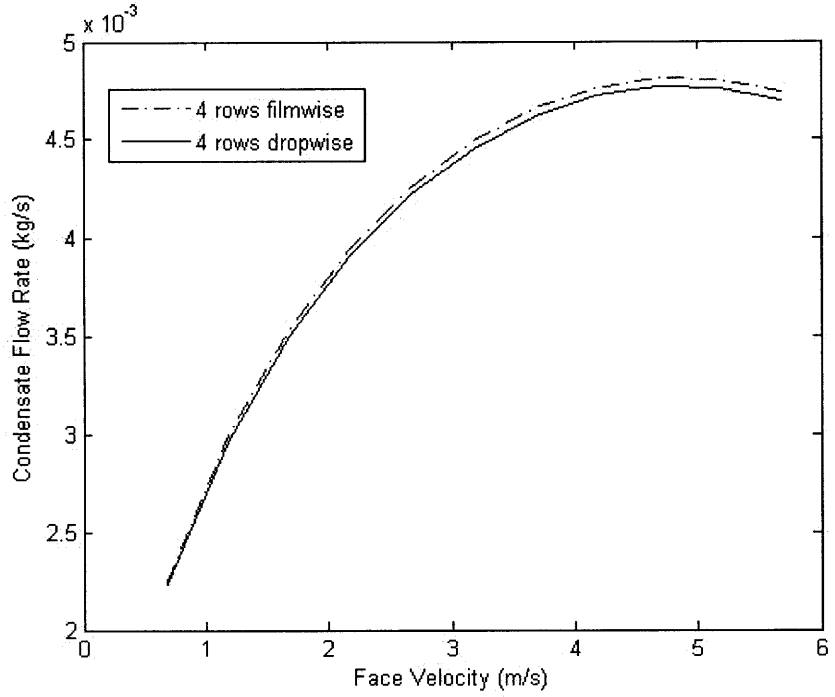

Figure 18: Condensate flow rate versus face velocity of air for dropwise and filmwise conditions.

Condensate flow rate versus face velocity of air curve shows that the condensate increases steadily as the face velocity of air increases until it reaches the peak value of the curve which is around 0.0048 kg/s at 4.6 m/s of face velocity. Then, the condensate flow rate curve slowly decreases and it was expected that the value of condensate flow rate could decrease almost to zero when the velocity of air is really high. The dropwise condition has slightly larger value for condensate flow rate since it has better mass and heat transfer coefficient. Nevertheless the difference is significantly small which less than 4.7 %.

5. Summary and Discussion

The numerical analysis by using simple heat exchanger and ε-NTU method for the dry condition of both finned tube condenser and cooling tubes predicted the temperature profile and humidity ratio profile of the condenser along the height of the condenser. The analysis could be a good estimation of air and water temperature at the condenser outlet. Although both condenser quite different in geometrical designs, the analysis somewhat shows that a condenser that has fins, performed better in thermal reaction especially in cooling process. Nevertheless, the dry analysis using the basic heat exchanger analysis was not able to comprehensively study the performance of a condenser.

The wet condition analysis on the plate-finned-tube condenser has provided with a lot of useful information on the parameters that influenced the performance of the condenser. Using *j factor* correlation, the analysis was able to study the effect of face velocity of air on heat and mass transfer coefficient, surface effectiveness and condensate flow rate. It also studies the effect of water velocity on the overall heat transfer coefficient of the system. As the face velocity of air increases, the heat and mass transfer coefficients of the system increases. Nevertheless, the surface effectiveness decreases as the face velocity increases. Another important point was that the overall heat transfer coefficient could be increased when the water velocity is increased. In addition, the 5 rows configuration for a plate finned tube condenser performed slightly better than the 4 rows configuration in terms of having better heat and mass transfer coefficients. This numerical analysis however might be prone to significant uncertainty since the process of finding the temperature outlet was based on calculation and reiteration process. Nevertheless, it is still a good approximation that can be used to compare with any experimental analysis.

6. Conclusions

In conclusion, numerical analysis using basic heat exchanger method and j-factor correlation method has found that face velocity of air, water velocity, number of rows of tube were some of the important parameters that control the performance of a condenser. An increase in number of rows, face velocity of air and water velocity can increase the heat and mass transfer coefficient. Nevertheless the surface effectiveness decreases when the face velocity increases. The numerical also shows that the condensate flow rate achieve its peak at certain value of face velocity before it decreases. With all the known important parameters, one could predict the heat transfer coefficient for a certain velocity and estimate how much amount of water that could be condensed with the condenser. This numerical estimation can still be improved in the future.

References

[1]ASHRAE Handbook. 1985 Fundamentals. SI Edition. American Society of Heating Refrigerating and Air Conditioning.Engineers. Inc.

[2]Chen, T.D. Conklin, J.C. Barker, V.D. Dehumidification: Prediction of Condensate Flow Rate for Plate-Fin Tube Exchangers using the Latent j-factor. 1999.

3Diaz, G. Yang, K.T. McClain, R.L. Heat Rate Predictions in Humid Air-Water Heat Exchangers using Correlations and Neural Networks.Vol 123 April 2001.

[4]Desowky H.T., Ethouney. H.M. Seawater Flowing Inside Tube Fundamentals of Sea Water Desalination.

[5]Lienhard IV, J.H., Lienhard V, J.H. "Forced Convection in a Variety of Configurations" Heat Transfer Textbook 3rd Ed. Cambridge, MA. p. 361

[6]McQuiston. Faye C., Parker. J.D. 1994. Heating, Ventilating, and Air Conditioning. John Wiley & Sons. New York 4th Ed.

[7]McQuiston, F. C., 1978, "Heat, Mass and Momentum Transfer Data for Five Plate Fin Tube Heat Transfer ," ASHRAE Trans., 84, Part 1, pp. 266-293.

[8]McQuiston, F. C., 1978, "Correlation of Heat, Mass and Momentum Transport Coefficients for Plate-Fin-Tube Heat Transfer Surfaces with Ctaggered Tubes," ASHRAE Trans., 84, Part 1, pp. 294-309

[9]Moran, Michael. J. Shapiro, Howard N. Fundamentals of Engineering Thermodynamics. 2nd Ed. John Wiley and Sons Inc. New York.

[10]Nawayseh Kh. N., Farid, M.M., Al-Hallaj, S., Al-Timimi, A.R., Solar Desalination Based on Humidification Process – I. Evaluating The Heat and Mass Transfer Coefficients. Energy Conversion & Management 40 (1999) 1423-1439.